

Guidelines for glaucoma imaging classification, annotation, and quality control for artificial intelligence applications

Wei-Hua Yang¹, Yan-Wu Xu^{2,3}, Xing-Huai Sun⁴, Expert Workgroup of Guidelines for Glaucoma Imaging Classification, Annotation, and Quality Control for Artificial Intelligence Applications

¹Shenzhen Eye Hospital, Shenzhen Eye Medical Center, Southern Medical University, Shenzhen 518040, Guangdong Province, China

²School of Future Technology, South China University of Technology, Guangzhou 510641, Guangdong Province, China

³Pazhou Lab, Guangzhou 510320, Guangdong Province, China

⁴Department of Ophthalmology & Visual Science, Eye & ENT Hospital, Shanghai Medical College, Fudan University, Shanghai 200031, China

Correspondence to: Wei-Hua Yang. Shenzhen Eye Hospital, Shenzhen Eye Medical Center, Southern Medical University, Shenzhen 518040, Guangdong Province, China. benben0606@139.com; Yan-Wu Xu. School of Future Technology, South China University of Technology, Guangzhou 510641, Guangdong Province, China. ywxu@iecc.org; Xing-Huai Sun. Department of Ophthalmology & Visual Science, Eye & ENT Hospital, Shanghai Medical College, Fudan University, Shanghai 200031, China. xhsun@shmu.edu.cn

Received: 2025-03-26 Accepted: 2025-05-26

Abstract

• Glaucoma is an eye disease characterized by pathologically elevated intraocular pressure, optic nerve atrophy, and visual field defects, which can lead to irreversible vision loss. In recent years, the rapid development of artificial intelligence (AI) technology has provided new approaches for the early diagnosis and management of glaucoma. By classifying and annotating glaucoma-related images, AI models can learn and recognize the specific pathological features of glaucoma, thereby achieving automated imaging analysis and classification. Research on glaucoma imaging classification and annotation mainly involves color fundus photography (CFP), optical coherence tomography (OCT), anterior segment optical coherence tomography (AS-OCT), and ultrasound biomicroscopy (UBM) images. CFP is primarily used for the annotation of the optic cup and disc, while OCT is used for measuring and annotating the thickness of the

retinal nerve fiber layer, and AS-OCT and UBM focus on the annotation of the anterior chamber angle structure and the measurement of anterior segment structural parameters. To standardize the classification and annotation of glaucoma images, enhance the quality and consistency of annotated data, and promote the clinical application of intelligent ophthalmology, this guideline has been developed. This guideline systematically elaborates on the principles, methods, processes, and quality control requirements for the classification and annotation of glaucoma images, providing standardized guidance for the classification and annotation of glaucoma images.

• **KEYWORDS:** glaucoma; artificial intelligence; classification; annotation; processes; quality control; guideline

DOI:10.18240/ijo.2025.07.01

Citation: Yang WH, Xu YW, Sun XH, *et al.* Guidelines for glaucoma imaging classification, annotation, and quality control for artificial intelligence applications. *Int J Ophthalmol* 2025;18(7):1181-1196

INTRODUCTION

Glaucoma is a chronic eye disease often associated with elevated intraocular pressure, which can lead to optic nerve damage and ultimately irreversible vision loss^[1]. Early symptoms of glaucoma are often subtle, making accurate and timely diagnosis crucial for preventing vision loss in patients. Based on underlying mechanisms, anatomical characteristics of the anterior chamber angle, and etiological factors, glaucoma can be further classified into several subtypes, including primary open angle glaucoma (POAG), primary angle-closure glaucoma (PACG), normal-tension glaucoma (NTG), secondary glaucoma, and congenital or juvenile glaucoma. POAG, the most common subtype, is characterized by an open anterior chamber angle with impaired aqueous outflow, while PACG involves structural narrowing or closure of the angle leading to obstructed drainage. NTG presents typical optic nerve damage despite normal intraocular pressure, suggesting individual susceptibility. Secondary glaucoma arises from other

ocular or systemic conditions such as trauma, inflammation, neovascularization, or medication-induced changes. Accurate identification of glaucoma subtypes is critical for personalized treatment planning and prognosis evaluation. With the rapid advancement of artificial intelligence (AI) in medicine, the diagnosis and management of ophthalmic diseases are increasingly moving towards precision and individualization. In the diagnosis and management of glaucoma, imaging, classification, and annotation provide essential data for AI models, offering significant potential for early screening and diagnosis. The classification and annotation of glaucoma images enable the accurate identification of characteristic structures, providing critical support for the training of AI algorithms. The combined use of various imaging techniques, including color fundus photography (CFP), optical coherence tomography (OCT), anterior segment optical coherence tomography (AS-OCT), and ultrasound biomicroscopy (UBM), not only enhances the accuracy of glaucoma diagnosis but also provides more imaging evidence for early detection and progression monitoring^[2].

Over the past decade, research in ophthalmic AI has shown significant growth, primarily focusing on the analysis and processing of ophthalmic imaging data using advanced computational methods^[3]. Existing guidelines for the clinical evaluation of AI in ophthalmology provide broad guidance for the application of AI technology in this field^[4-5]. However, for the specific disease of glaucoma, there remains a lack of unified technical standards and standardized operational methods, which limits the accuracy and generalizability of AI models^[6]. To address these issues, we have organized a panel of clinical experts, imaging specialists, and AI researchers to form the Expert Workgroup for the Guidelines for Glaucoma Imaging Classification, Annotation, and Quality Control for Artificial Intelligence Applications. In early 2023, the workgroup conducted an in-depth investigation into the current state of glaucoma imaging annotation in China, identifying major issues in clinical practice and research, as well as technical needs in annotation practices.

During the development of this guideline, the expert panel reviewed relevant domestic and international literature, organized expert discussions and iterative reviews, and detailed the key technical points of glaucoma imaging classification and annotation. The workgroup drafted the initial guideline based on these discussions, solicited feedback from experts via email and WeChat, and revised and refined the document repeatedly before finalizing it. The development of this guideline took approximately two years. The guideline aims to provide standardized operational guidance for the classification and annotation of glaucoma images, improving the quality and consistency of imaging data, thereby promoting the application

of AI technology in the early diagnosis and management of glaucoma.

COMMON IMAGING MODALITIES AND TASKS IN GLAUCOMA IMAGING CLASSIFICATION AND ANNOTATION

The goal of glaucoma classification and annotation is to accurately annotate different types of fundus images, enabling computer vision systems to learn and understand the ocular structures and pathologies associated with glaucoma, thereby achieving automated diagnosis and analysis of the disease^[7]. The following outlines the research scope and tasks for different glaucoma imaging modalities:

CFP Research scope: annotation of the optic cup and disc in CFP, and classification. Task: by annotating the boundaries, morphology, and color features of the optic cup and disc, achieve glaucoma diagnosis and monitor changes in the optic disc.

OCT Research scope: measurement and annotation of the retinal nerve fiber layer (RNFL) in OCT images. Task: annotate the thickness, morphology, and abnormalities of the RNFL for early glaucoma diagnosis and disease progression monitoring.

AS-OCT Research scope: annotation of the anterior chamber angle and parameter calculation in AS-OCT images. Task: annotate structures such as the iris root and trabecular meshwork to assess the anatomical structure of the anterior chamber angle, aiding in glaucoma diagnosis and treatment.

UBM Research scope: annotation of the anterior chamber angle and parameter calculation in UBM images. Task: Annotate structures such as the anterior chamber angle, iris root, ciliary body, and sclera to obtain detailed anatomical information on the angle, supporting the understanding of glaucoma pathogenesis.

PRINCIPLES AND METHODS OF GLAUCOMA IMAGING CLASSIFICATION AND ANNOTATION

Principles of Glaucoma Imaging Classification

Classification of glaucoma in CFP Glaucoma is a chronic degenerative optic neuropathy characterized by the loss of retinal ganglion cells (RGCs) and their axons^[8]. In CFPs, characteristic changes in the optic cup/disc and loss of the neuroretinal rim can often be observed^[9].

1) Cup-to-disc ratio enlargement Glaucoma often leads to changes in the shape, color, and depth of the optic cup and disc. In CFPs, the expansion of the bright central area of the optic cup and the typical optic disc cupping of glaucoma can be observed^[10]. The optic disc is a structural region in the fundus located at the posterior part of the eye, where the optic nerve exits the eyeball. The optic disc typically appears as a round or oval structure with a pale red hue. The optic cup is the central depression within the optic disc, appearing as a bright,

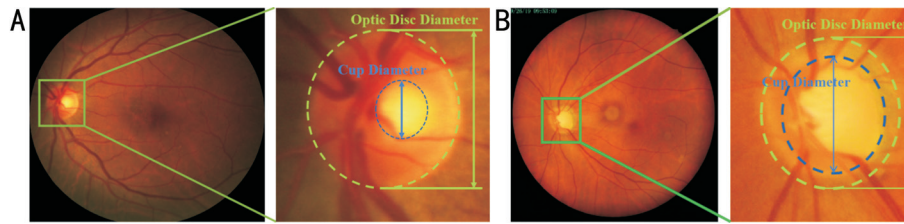


Figure 1 CDR in normal and glaucomatous CFPs A: CDR in a normal CFP; B: CDR in a glaucomatous CFP. CDR: Cup-to-disc diameter ratio; CFP: Color fundus photography.

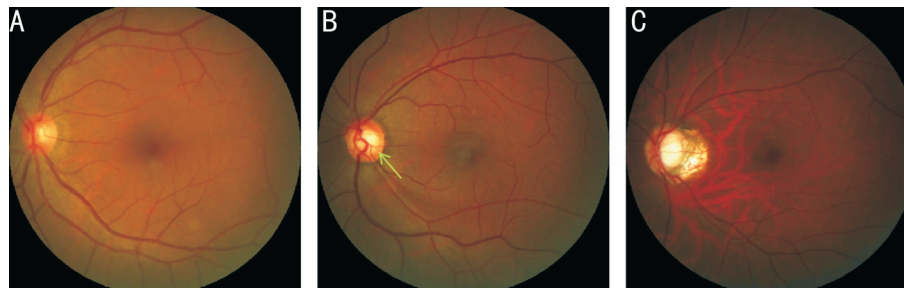


Figure 2 Comparison of normal CFPs with abnormal optic disc rim A: Normal CFP; B: CFP with localized loss of the optic disc rim, showing atrophy in a specific area of the disc margin; C: CFP with diffuse loss of optic disc rim tissue, showing widespread atrophy along the disc margin. CFP: Color fundus photography.

round or oval area. The optic cup and disc overlap, but the area of the optic cup is smaller than that of the optic disc^[11]. Figure 1 illustrates the difference in cup-to-disc ratio (CDR) between normal and glaucomatous CFPs, showing that the CDR in glaucomatous images is larger than in normal images.

Clinically, the CDR is determined by the vertical cup diameter (VCD) and the vertical disc diameter (VDD). The formula for CDR is as follows:

$$CDR = \frac{VCD}{VDD}$$

Generally, a CDR greater than 0.6 in CFPs suggests a potential risk of glaucoma^[12].

2) Neuroretinal rim abnormalities Loss of neuroretinal rim tissue or abnormal rim thickness may be associated with the progression of glaucoma^[13]. Figure 2 illustrates normal CFPs with different types of rim loss. Focal loss is characterized by notching or pseudo-excavation in the temporal region of the superior and inferior poles of the optic disc, accompanied by vessel kinking^[14]. Diffuse rim loss appears as a moth-eaten pattern with a pale color and prominent peripapillary atrophy^[15].

3) Violation of the ISNT rule In normal CFPs, the neuroretinal rim typically follows the ISNT rule^[16], where the inferior rim is the widest, followed by the superior, then the nasal, and the narrowest temporal (Figure 3). Specifically, the rim width distribution follows: inferior > superior > nasal > temporal. This pattern is significant for identifying abnormal changes in the optic disc, particularly rim loss due to glaucoma. If the rim width does not follow the ISNT rule, such as the inferior rim being narrower than the nasal rim or the nasal rim being wider than expected, glaucoma should be considered.

Classification of glaucoma in OCT images Due to the dynamic changes in the inner retinal structures caused by glaucoma and the logarithmic relationship affecting visual field threshold sensitivity, clinical visual field defects are only observable after 40%-50% of RGCs are lost^[17]. However, OCT can detect subtle changes in the inner retinal layers and is not affected by patient cooperation, making it valuable for early diagnosis of glaucomatous damage. OCT can diagnose glaucoma even before visual field defects occur, a condition known as pre-perimetric glaucoma. In recent years, OCT has been increasingly used in the clinical diagnosis and management of glaucoma, primarily for monitoring the RNFL and optic disc^[18].

1) RNFL thinning RNFL thinning can be observed in OCT images even before changes in the optic disc or visual field occur^[19]. OCT allows for quantitative observation of the RNFL, enabling earlier detection of RNFL damage. In normal eyes, the average RNFL thickness is around 100 μm, with thinner regions (approximately 70 μm) on the temporal and nasal sides and thicker regions (120-130 μm) superiorly and inferiorly. Figure 4 shows OCT images of a normal eye^[20]. Alasil *et al*^[21] found that in POAG patients, the critical points for significant visual field damage were an average RNFL thickness of 89 μm, superior thickness of 100 μm, and inferior thickness of 73 μm.

2) Optic disc cupping and cup enlargement Radial scans centered on the optic disc can clearly show the optic disc contour, cupping, and the surrounding RNFL^[22]. In OCT images, the degree of optic disc cupping and cup enlargement can be quantitatively measured^[23]. A CDR greater than 0.6 suggests a potential risk of glaucoma. Figure 5 illustrates the difference in CDR between normal and glaucomatous eyes.

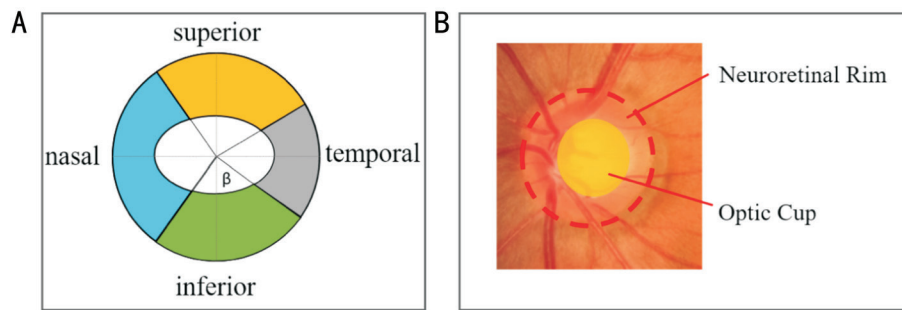


Figure 3 Schematic diagram of the ISNT rule The ISNT rule refers to the typical order of neuroretinal rim thickness in a healthy optic disc: inferior > superior > nasal > temporal. A: Schematic diagram of the optic disc divided into four quadrants: nasal (N), superior (S), temporal (T), and inferior (I); B: Schematic diagram of the optic disc structure, showing the positional relationship between the disc rim and the optic cup.

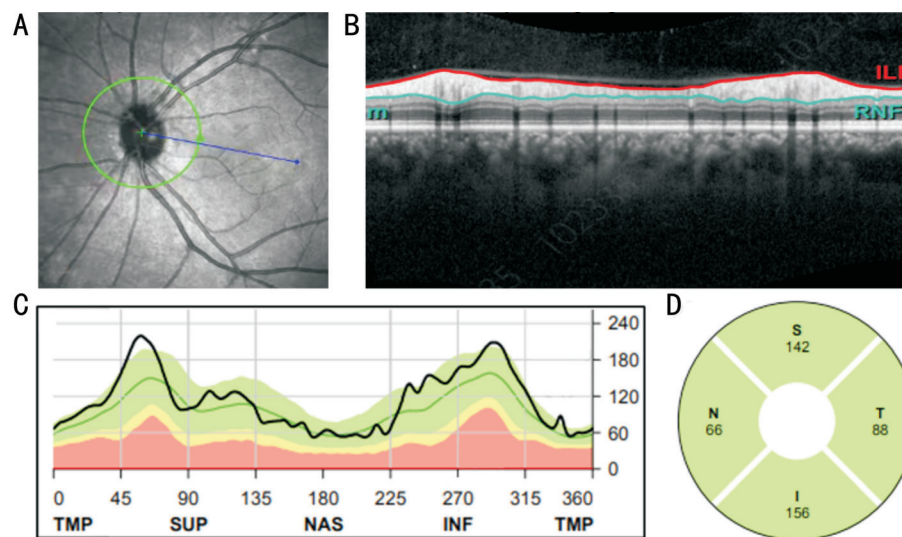


Figure 4 Optical coherence tomography (OCT) image and analysis of normal retinal nerve fiber layer (RNFL) A: OCT scan of the optic disc and peripapillary region; B: Unfolded image of the internal limiting membrane (ILM) and retinal nerve fiber layer (RNFL), corresponding to the position of the circle (green) in the OCT infrared scan. These two lines represent the boundaries of the peripapillary RNFL (pRNFL); C: Thickness distribution of the pRNFL corresponding to the circle (green), categorized into normal (green/top = normal, yellow/middle = borderline, red/bottom = pathological); D: Sample of average pRNFL thickness in different sectors.

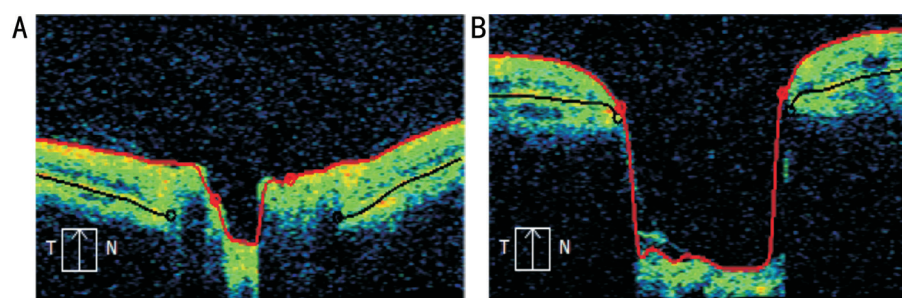


Figure 5 CDR in normal individuals and glaucoma patients A: CDR in a normal individual; B: CDR in a glaucoma patient. The horizontal distance of the red circle represents the diameter of the optic cup, while the horizontal distance of the black circle represents the diameter of the optic disc. CDR: Cup-to-disc diameter ratio.

Classification of glaucoma in anterior segment imaging

The anterior segment, located anterior to the lens, includes the cornea, sclera, anterior chamber, iris, pupil, and lens^[24]. AS-OCT and UBM can clearly display the cross-sectional morphology of the anterior segment structures, which are crucial for glaucoma diagnosis and treatment^[25]. Figure 6 shows AS-OCT and UBM images of the anterior chamber

angle, with AS-OCT providing complete imaging of the angle and UBM offering better visualization of deeper structures such as the ciliary body and lens. Figure 7 illustrates the anatomy of the anterior chamber angle, aiding in understanding its features. Analysis of glaucoma using AS-OCT and UBM primarily focuses on the anterior chamber angle and iris status.

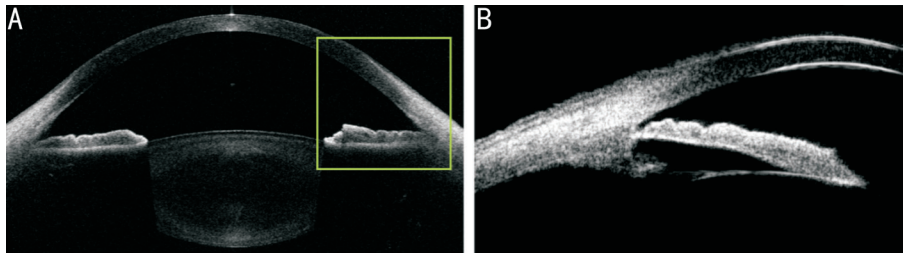


Figure 6 Cross-sectional morphology of anterior segment structures A: Image obtained using anterior segment optical coherence tomography (AS-OCT); B: Image obtained using ultrasound biomicroscopy (UBM).

1) POAG vs PACG In the United States, the most common type of glaucoma is POAG, while in other regions, PACG is the predominant type^[26-28]. The pathogenesis of POAG is not fully understood, but it may be related to dysfunction or structural damage of the trabecular meshwork, leading to increased aqueous production or impaired outflow^[29]. PACG is caused by the narrowing of the anterior chamber angle between the iris and cornea, blocking aqueous outflow and leading to elevated intraocular pressure and optic nerve damage^[30]. Figure 8 shows AS-OCT images of POAG and PACG. Patients with POAG and PACG exhibit significant structural differences in the anterior chamber angle and ocular biometric parameters, including a narrow anterior chamber angle, shorter axial length, and thicker lens^[30]. In POAG images, the anterior chamber angle entrance appears wide, the iris is flat, and all structures of the anterior chamber angle are visible. In contrast, PACG images show a narrow anterior chamber angle entrance, peripheral iris bombe, and all or part of the structures in the anterior chamber angle are not visible.

2) PACG grading Anterior chamber angle grading involves numerical classification of the angle width (degree of openness) to assess the risk of angle closure. Common grading methods include the Scheie^[31], Shaffer^[32], van Herick^[33] and Spaeth grading systems^[34]. The Scheie method grades the angle based on the visibility of anatomical structures such as the ciliary body band, iris, trabecular meshwork, and Schwalbe's line. The van Herick method assesses the peripheral anterior chamber depth (ACD) relative to corneal thickness, with a depth less than one-quarter of the corneal thickness indicating a risk of angle closure. The Spaeth method is the most detailed and complex, considering the angle width, peripheral iris morphology, and iris root attachment. The Shaffer grading system, the most widely used internationally, classifies the angle based on the width of the angle between the corneal-trabecular meshwork surface and the peripheral iris surface (Figure 9; Table 1).

3) Acute vs chronic PACG The clinical manifestations of PACG are complex and can be categorized into acute and chronic forms.

a) Acute PACG: in imaging of the anterior segment, a

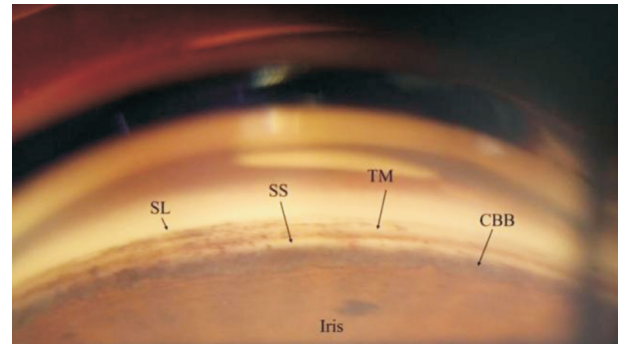


Figure 7 Schematic diagram of the anterior chamber angle structures SL: Schwalbe's line; SS: Scleral spur; TM: Trabecular meshwork; CBB: Ciliary body band.

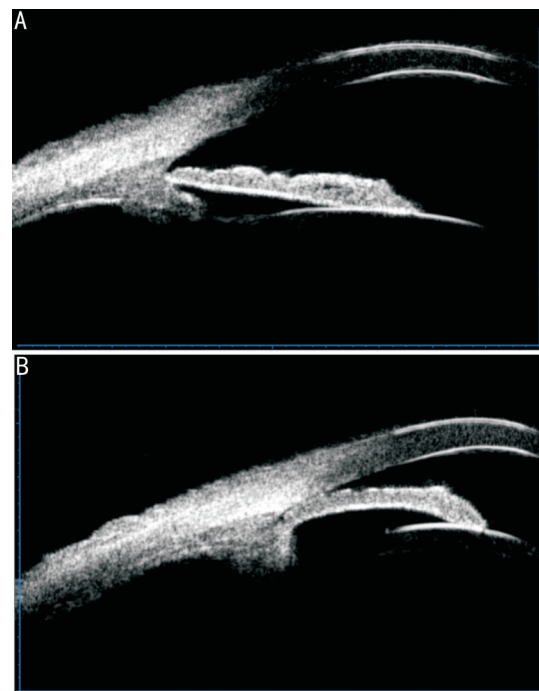


Figure 8 Ultrasound biomicroscopy (UBM) images of the anterior chamber angle in glaucoma A: UBM image of the anterior chamber angle in open angle glaucoma (OAG), showing an open angle and a flat iris; B: UBM image of the anterior chamber angle in angle-closure glaucoma (ACG), showing a closed angle and forward bowing of the iris.

markedly bulging iris with a narrow anterior chamber angle is often observed. The angle closure occurs in an “all-or-none” manner, with varying degrees of severity, and the angle closure

Table 1 Shaffer grading system criteria

| Anterior chamber angle width | Description of anterior chamber angle | Angle grade | Judgment of angle closure |
|------------------------------|---------------------------------------|-------------|------------------------------------|
| 35°-45° | Wide open | 4 | Closure impossible |
| 20°-35° | Wide open | 3 | Closure impossible |
| 10°-20° | Moderately narrow | 2 | Closure possible |
| ≤10° | Very narrow | 1 | Suspected angle closure |
| Slit or closed | Slit-like or closed | 0 | Closure imminent or already closed |

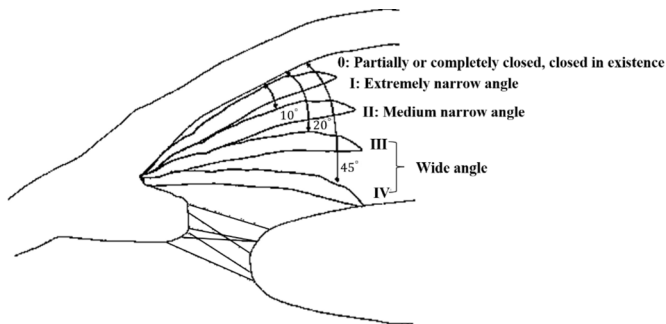


Figure 9 Schematic diagram of the shaffer grading method
According to the Shaffer grading system, the angle width ranges from 0 to 45°. Generally, an angle width less than 20° (narrow, beak-like) suggests a potentially closable narrow angle, while an angle width less than 10° indicates a high-risk narrow angle requiring further evaluation.

is sudden and extensive^[29]. Figure 10 illustrates iris bombe caused by pupillary block.

b) Chronic PACG: primary chronic angle-closure glaucoma shares similar anatomical features with primary acute angle-closure glaucoma, such as microphthalmos, small cornea, short axial length, thick lens, and shallow anterior chamber. It progresses chronically, with the anterior chamber angle narrowing until complete closure, leading to a gradual increase in intraocular pressure^[35]. Unlike acute angle-closure glaucoma, there is no associated pupillary dilation or iris atrophy. Chronic angle-closure glaucoma emphasizes optic nerve damage and visual field defects. The pathogenesis of primary chronic angle-closure glaucoma is not fully understood, and UBM often shows a high iris plateau configuration or mixed mechanisms^[29]. Figure 11 demonstrates the UBM findings of two mechanisms in primary chronic angle-closure glaucoma.

4) Classification based on anterior chamber angle structural parameters Analysis of AS-OCT or UBM images allows for precise measurement of anterior chamber angle structural parameters. These measurements can help determine whether a patient has PACG. Commonly used parameters include the trabecular iris angle (TIA), angle opening distance (AOD), and angle recess area (ARA)^[36-38]. Figure 12 illustrates the annotation of anterior chamber angle parameters on a UBM image. Table 2 lists the parameters related to anterior segment anatomy and their correlation with glaucoma. Among these parameters, ACD has better screening performance than

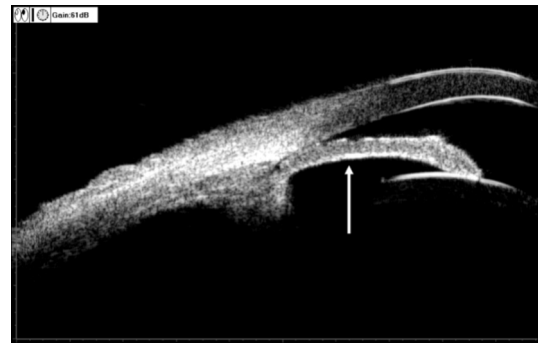


Figure 10 Acute primary angle-closure glaucoma (PACG) Ultrasound biomicroscopy (UBM) of this case shows iris bombe due to high posterior chamber pressure (white arrow), leading to mechanical closure of the anterior chamber angle.

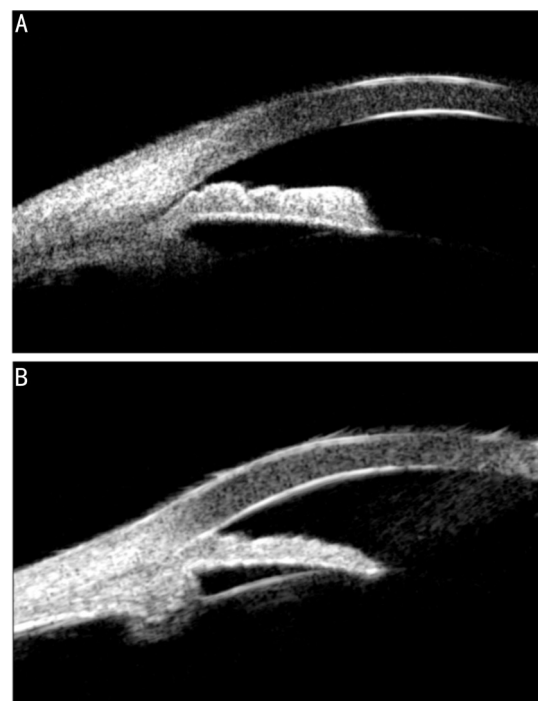


Figure 11 Chronic primary angle-closure glaucoma (PACG) A: Ultrasound biomicroscopy (UBM) showing high iris plateau configuration; B: UBM showing peripheral iris thickening.

iris parameters such as iris thickness (IT) and iris curvature (I-CURV). Specifically, iris parameters alone are insufficient for identifying narrow anterior chamber angles. TIA is a more sensitive indicator of anterior chamber angle openness than AOD.

Structural Annotation Principles and Methods in Glaucoma Imaging

Optic cup and disc annotation in CFP Glaucoma is

Table 2 Anterior segment anatomical parameters and their correlation with glaucoma

| Parameter type | Parameter name | Parameter description | Correlation |
|-----------------------------------|----------------|---|--------------------------|
| Iris parameters | IT | The distance between the anterior and posterior surfaces of the iris, measured at a point 500 μm , 750 μm , or 2000 μm from the SS on the anterior iris surface. A perpendicular line is drawn from this point to the posterior iris surface, and the distance between the two intersection points is defined as IT. | Positive ^[27] |
| | I-CURV | The vertical distance from the highest point of the posterior iris curvature to the reference line connecting the most peripheral and central points of the iris pigment epithelium. | Positive ^[28] |
| Anterior chamber parameters | ACD | The space between the posterior surface of the cornea and the anterior surface of the lens, including the central anterior chamber depth (cACD) and the peripheral anterior chamber depth (pACD). | Negative ^[29] |
| | ACA and ACV | ACA is the cross-sectional area enclosed by the corneal endothelium, the anterior iris surface, and the anterior lens surface within the pupil. ACV is the volume formed by rotating the ACA around the line connecting the corneal reflection point and the apex of the lens through 360°. | Negative ^[30] |
| Anterior chamber angle parameters | AOD | The distance between two points where a line perpendicular to the cornea intersects the trabecular meshwork at 500 μm or 750 μm from the SS and the anterior iris surface. | Negative ^[31] |
| | ARA and TISA | ARA is defined as the area enclosed by the AOD, the anterior surface of the iris, and the posterior surface of the cornea. TISA is the area bounded by four specific boundaries: the posterior boundary is the line connecting the SS and the intersection point of a perpendicular line drawn from the SS to the iris; the anterior boundary is the AOD; the upper boundary is the inner wall of the corneoscleral limbus between the anterior and posterior boundaries; and the lower boundary is the iris surface between the anterior and posterior boundaries. These four boundaries collectively define the TISA. | Negative ^[32] |
| | TIA | TIA is calculated as follows: a circle with a radius of 500 μm is drawn with the SS as its center. This circle intersects the corneal endothelium and the anterior surface of the iris. The angle formed at the SS by the two lines connecting the SS to these intersection points is defined as the TIA. | Negative ^[33] |

Positive correlation indicates that a higher parameter value increases the likelihood of glaucoma, while negative correlation indicates the opposite. ACD: Anterior chamber depth; ACA: Anterior chamber area; ACV: Anterior chamber volume; TIA: Trabecular iris angle; AOD: Angle opening distance; ARA: Angle recess area; TISA: Trabecular iris space area; IT: Iris thickness; I-CURV: Iris curvature; SS: Scleral spur.

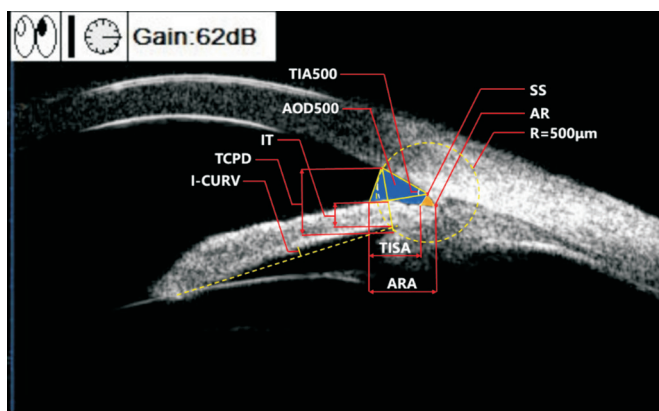


Figure 12 Annotation of anterior chamber angle parameters on a ultrasound biomicroscopy (UBM) image '500' after the parameter refers to the measured marker distance SS 500 μm . TCPD: Trabecular ciliary process distance; AR: Angle recess; TISA: Trabecular iris space area; TIA: Trabecular iris angle; AOD: Angle opening distance; IT: Iris thickness; I-CURV: Iris curvature; ARA: Angle recess area; SS: Scleral spur.

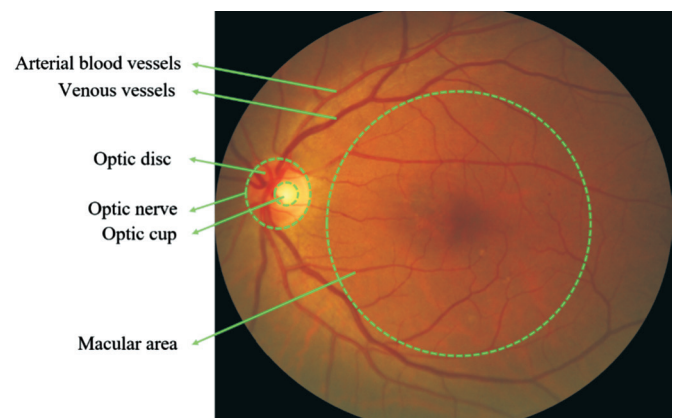


Figure 13 Basic structure of the fundus in CFP The location of the macular region is referenced according to the guidelines issued by the Retinal Disease Group of the Chinese Ophthalmological Society^[41]. CFP: Color fundus photography.

a common eye disease characterized by pathological enlargement of the optic cup due to increased intraocular pressure, which compresses the optic nerve head (optic disc) and its vessels^[39]. The optic disc is a pale red, circular structure in the fundus where the optic nerve exits the eye. The optic cup is the central depression within the optic disc. Since the optic disc and cup share similar color and brightness, with no clear boundary, manual annotation is often required to delineate their edges^[40]. Figure 13 shows the basic structure of a color fundus photograph^[41]. The following principles should be followed when annotating the optic cup and disc.

- 1) Identify the optic disc location: The optic disc is a pale red, disc-shaped structure located slightly nasal to the posterior pole of the eyeball. Annotators can use this information to locate the optic disc.
- 2) Define the optic disc edge: The optic disc typically appears lighter in color compared to the surrounding retinal tissue, which is darker. By observing color contrasts and variations, the boundary of the optic disc can be delineated.
- 3) Identify the optic cup location: The optic cup is located within the optic disc and appears as a brighter region compared to the surrounding optic disc and RNFL, creating a color contrast.
- 4) Define the optic cup edge: The edge of the optic cup can be determined by analyzing the color and brightness contrasts between the optic cup and the surrounding neuroretinal rim.

Retinal layer annotation in OCT imaging Many ocular diseases cause changes in the thickness of the retinal and choroidal layers, with severe cases leading to the degeneration or disappearance of certain cell layers. For example, glaucoma causes thinning of the RNFL^[42-43]. OCT is a non-contact, non-invasive imaging technique that provides detailed cross-sectional images of the retina, allowing for precise anatomical analysis. OCT scans can be centered on the fovea (macular scan) or the optic disc^[44]. Figure 14 shows a wide-angle OCT scan covering both the macular and optic disc regions.

Layer segmentation of OCT images enables quantitative analysis of retinal layer thickness and its correlation with disease. In clinical practice, manual annotation of retinal layers is often required. Figure 15 illustrates an OCT image centered on the fovea and its manual layer annotation.

When diagnosing glaucoma, annotators must clearly distinguish different retinal layers, especially the RNFL, and measure its thickness to monitor glaucoma progression. The following principles should be followed.

- 1) Locate the optic nerve head (optic disc): The RNFL converges at the optic disc, so its location must be accurately identified.
- 2) Locate the macula: If the image is acquired from a scan centered on the macula, the macular region must be annotated. The macula is a central structure of the retina that is closely associated with visual acuity.
- 3) Annotate the RNFL edges: The inner and outer boundaries of the RNFL should be annotated to measure its thickness.
- 4) Segment and measure RNFL thickness: As required, the OCT image can be segmented, typically into distinct sectors such as superior, inferior, temporal, nasal, or other fan-shaped regions. Measure the RNFL thickness within each localized area and then calculate the average or other relevant metrics.

Anterior chamber angle annotation in AS-OCT and UBM Imaging The anterior chamber angle, the primary pathway for aqueous humor drainage, is the angle formed between the iris root and the cornea, consisting of anterior and posterior walls and the recess between them^[45]. The anatomical structure of the anterior segment and anterior chamber angle is shown in Figure 16. The anterior chamber angle plays a vital role in aqueous humor outflow, and its obstruction can lead to increased intraocular pressure, ultimately resulting in glaucoma. Anterior chamber angle assessment is crucial for glaucoma diagnosis and treatment evaluation, and its visualization is essential for accurate assessment. Current visualization techniques include AS-OCT and UBM.

AS-OCT and UBM provide clear meridional cross-sectional views of the anterior chamber angle, enabling quantitative measurement of angle opening parameters such as TIA, AOD, and ARA. These measurements rely on the identification of specific anatomical landmarks, particularly the scleral spur



Figure 14 Example of a wide-angle OCT scan OCT: Optical coherence tomography.

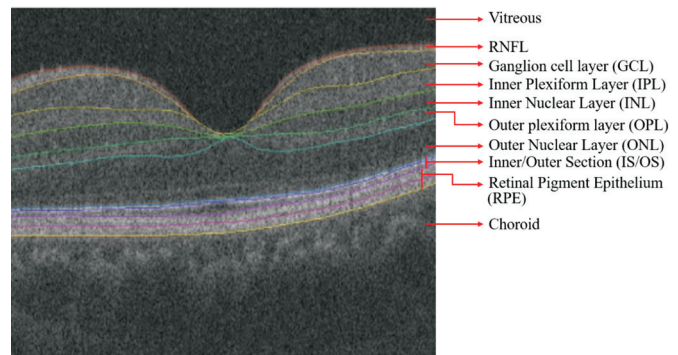


Figure 15 A B-scan of a macular-centered retinal OCT image and a schematic of layer annotation for fundus structures OCT: Optical coherence tomography.

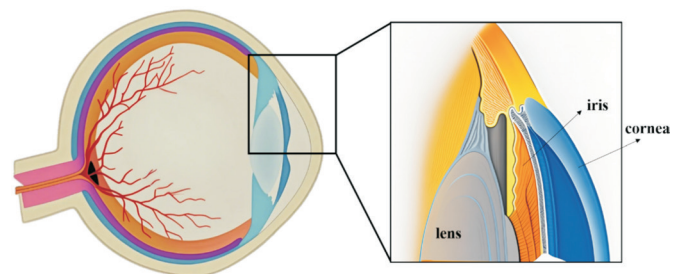


Figure 16 Schematic diagram of the anatomical structure of the anterior chamber angle.

(SS), the junction point of the posterior corneal curvature and the scleral curvature, located posterior to the iris root and ciliary body^[30]. In cross-sectional images, the SS appears as a wedge-shaped protrusion from the inner scleral surface, as shown in Figure 17.

SS located approximately 500 μm anterior to the inner scleral surface, encompasses the entire trabecular meshwork, the primary pathway for aqueous humor outflow. Since the trabecular meshwork is difficult to distinguish in AS-OCT and UBM images, the trabecular meshwork point should be marked as another key landmark. The aqueous recess is the region where aqueous humor flows, appearing as a recessed area in imaging, and is used to annotate the angle recess (AR) position to assess the depth and structure of the anterior chamber angle^[46]. Using these three points as reference landmarks, various anterior chamber angle opening parameters can be annotated and calculate^[47]. Figure 18 illustrates the annotation of these parameters in AS-OCT imaging, including the crystalline lens rise (CLR), an important parameter for evaluating the position of the lens, defined as the vertical

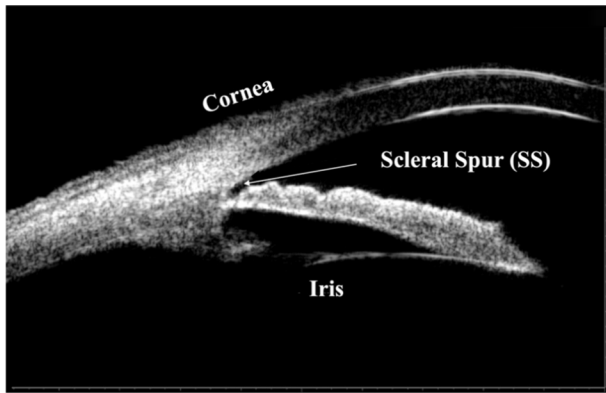


Figure 17 Location of the SS point in the cross-sectional view SS: Scleral spur.

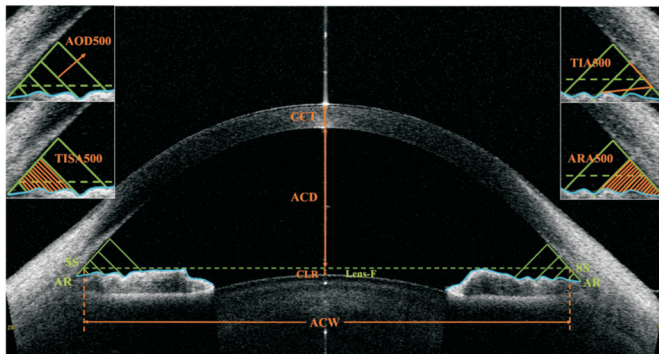


Figure 18 Schematic diagram of anterior segment parameters '500' after the parameter refers to the measured marker distance SS 500 μm . ACW: Anterior chamber width; CLR: Crystalline lens rise; ACD: Anterior chamber depth; TIA: Trabecular iris angle; AOD: Angle opening distance; ARA: Angle recess area; TISA: Trabecular iris space area.

distance from the anterior pole of the lens to the horizontal line connecting the two SS points. The following principles guide the annotation of the anterior chamber angle.

- 1) Identify image structures: First, accurately identify structures related to the anterior chamber angle, including the corneal endothelium, trabecular meshwork, iris root, and angle recess. Ensure image clarity to make these structures discernible.
- 2) Locate the SS and trabecular meshwork points: Identify the SS and the trabecular meshwork point located 500 μm from the SS.
- 3) Locate the augmented reality (AR) point: Identify and mark the angle recess point.
- 4) Measure anterior chamber angle parameters: Use software tools to measure parameters such as AOD500 and TIA500, which are useful for assessing the width and depth of the anterior chamber angle.
- 5) Multi-angle measurements: Perform measurements in different directions to obtain comprehensive information about the anterior chamber angle structure, aiding in a thorough understanding of its morphology.

PROCESS OF GLAUCOMA IMAGING CLASSIFICATION AND ANNOTATION

The standardization of the process for annotating ocular structures in glaucoma imaging is crucial to ensure consistency,

comparability, and accuracy^[48]. Below are some general procedures for the classification and annotation of glaucoma images.

- 1) Qualification requirements for classifiers and annotators: Classifiers and annotators should possess a medical background in ophthalmology or optometry, with a thorough understanding of the clinical features of glaucoma and related imaging manifestations. They should have experience in interpreting CFPs, AS-OCT, UBM, OCT, and other relevant technologies.
- 2) Image screening and preprocessing: Ensure the use of high-quality ophthalmic images. Discard images with treatment traces or those that are unreadable. Inspect images to eliminate any artifacts or interference, ensuring the image quality meets the required standards.
- 3) Structure identification: Accurately identify and mark key structures in the images, including the retina, optic disc, macula, anterior chamber angle, trabecular meshwork, iris root, and others.
- 4) Classification and annotation of glaucoma images: Mark regions relevant to glaucoma diagnosis on images from various modalities and determine the presence and type of glaucoma.
- 5) Annotation of abnormal areas: Annotate any abnormal areas, such as breaks, defects, thinning, *etc.*, which may be associated with glaucoma or other ocular diseases.
- 6) Data recording and reporting: Record all measurement results, including structural parameters and abnormal areas. Generate standardized reports as needed to help physicians and other healthcare professionals better understand the patient's ocular condition.
- 7) Consistency and standardization: Adhere to principles of consistency and standardization to ensure that annotation results are comparable across different physicians or devices.

Standardization Recommendations for Glaucoma Imaging Classification and Annotation Procedures

Fundus imaging classification and annotation workflow

Figure 19 illustrates the workflow for the classification and annotation of CFPs: 1) Conduct an initial screening of the CFPs to assess image quality, excluding blurred or unclear images. 2) Annotate the positions of the optic cup and optic disc. 3) Determine the presence of glaucoma and assess the risk of glaucoma based on the CDR and neuroretinal rim characteristics.

Anterior segment imaging classification and annotation workflow

Figure 20 demonstrates the workflow for the classification and annotation of anterior segment images: 1) Perform an initial screening of AS-OCT/UBM images to ensure image quality and clarity. 2) Focus on the anterior chamber angle region in AS-OCT/UBM images and measure parameters such as TIA, AOD, and ARA. 3) Classify the morphology of the anterior chamber angle based on the measured parameters and image features, using a grading system. 4) For angle-closure glaucoma, annotate the clinical manifestations, including features of acute and chronic angle-closure glaucoma.

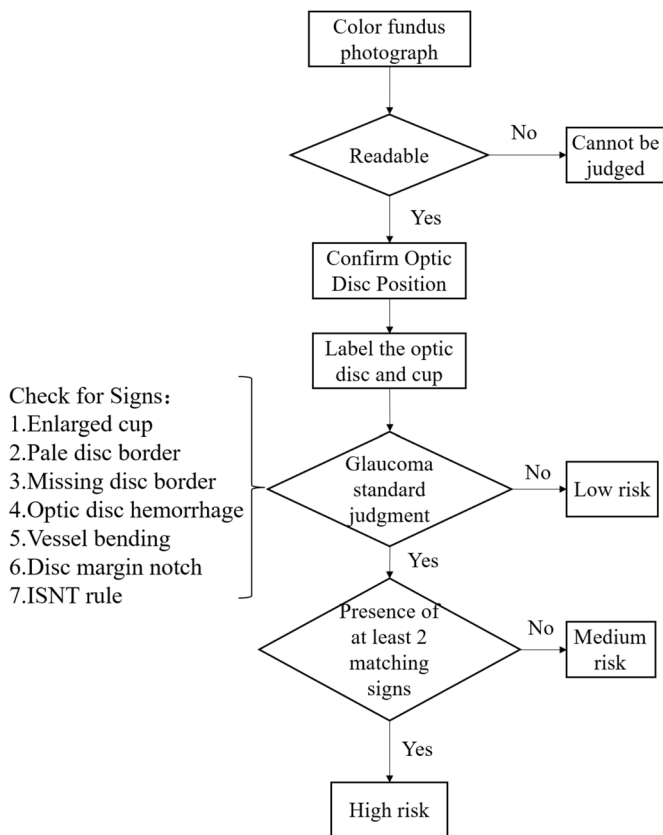


Figure 19 Workflow for fundus imaging classification and annotation ISNT rule: Inferior-superior-nasal-temporal rule.

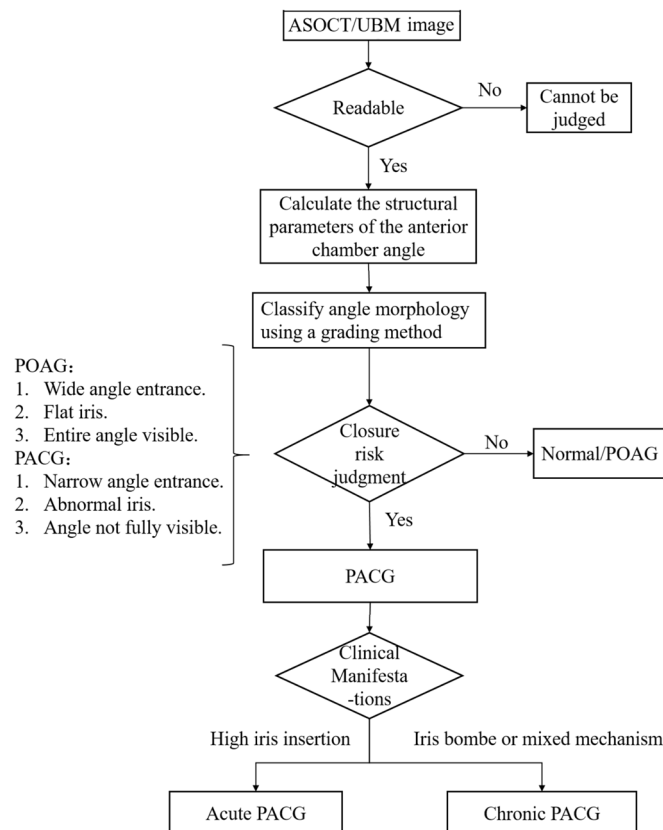


Figure 20 Workflow for anterior segment imaging classification and annotation ASOCT: Anterior segment optical coherence tomography; UBM: Ultrasound biomicroscopy; PACG: Primary angle-closure glaucoma; POAG: Primary open angle glaucoma.

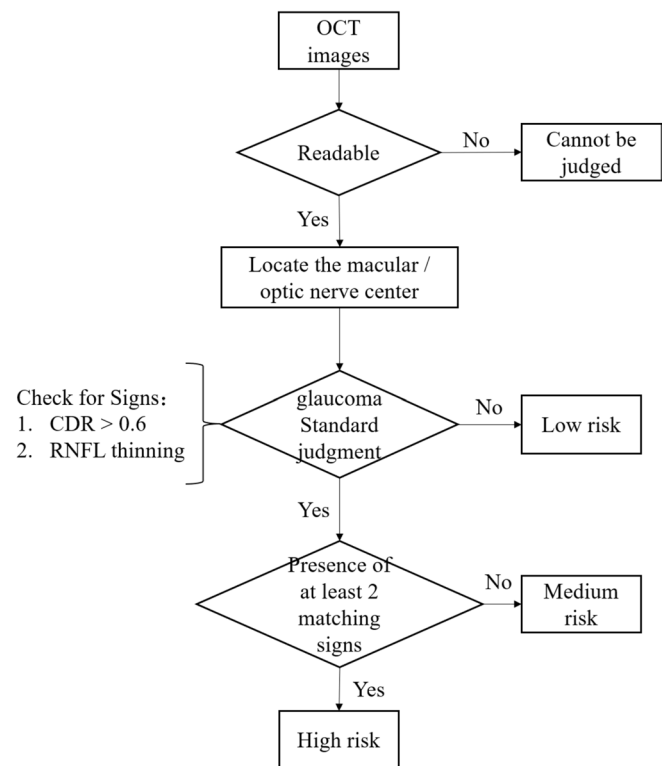


Figure 21 Workflow for OCT imaging classification and annotation OCT: Optical coherence tomography; CDR: Cup-to-disc diameter ratio; RNFL: Retinal nerve fiber layer.

Glaucoma OCT Imaging Classification and Annotation

Workflow Figure 21 outlines the workflow for the classification of OCT images: 1) Perform a quality check on OCT images, excluding unclear or artifact-affected images. 2) Determine the scanning mode of the OCT images: macular-centered or optic disc-centered scans. 3) Annotate changes in RNFL thickness, indicating the presence of early damage. 4) Annotate the degree of optic disc cupping and optic cup enlargement, comparing them with OCT images of normal eyes.

Standardization Recommendations for Structural Annotation in Glaucoma Imaging

The annotation of structures in glaucoma imaging can be conducted using self-developed annotation software or open-source medical imaging and general-purpose annotation tools such as MD.ai, 3DSlicer, ITK-SNAP, and LabelImg. Regardless of the annotation method employed, it is essential to adhere to standardized annotation procedures.

Annotation procedure for optic cup and optic disc in CFP

The primary observation area for the annotation of the optic cup and optic disc in CFP is a localized region within two optic disc diameters. The main annotation procedure is illustrated in Figure 22 and includes the following steps.

- 1) Image quality assessment: Ensure the image quality is suitable for accurate annotation.
- 2) Optic disc annotation: The annotator must delineate the edges of the optic disc, typically

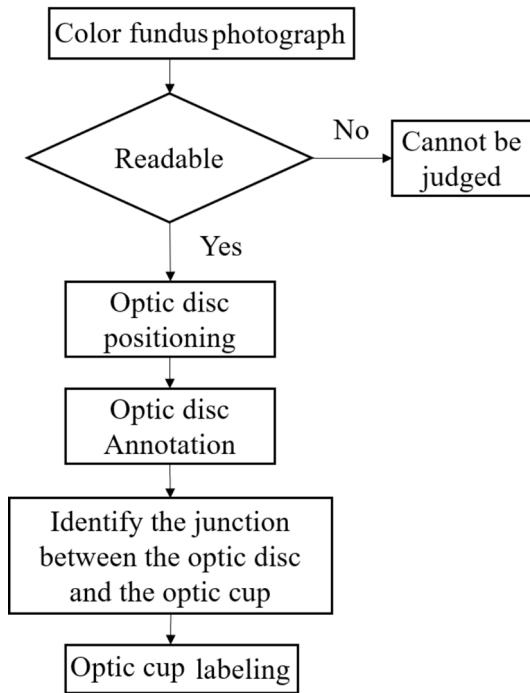


Figure 22 Annotation procedure for optic cup and disc in color fundus photography.

identified by the color transition around the optic nerve head (optic disc). Careful observation is required to accurately outline the disc margins, ensuring precision in the annotation. 3) Identification of the optic disc-cup junction: There exists a transitional zone between the optic disc and the optic cup, where the edges of the disc and cup meet. The annotator must precisely mark this boundary to provide detailed structural information. 4) Optic cup annotation: The optic cup is the central depression within the optic disc, and its shape and size vary among individuals. The annotator must determine the edges of the cup, distinguishing them from the disc margins. Accurate delineation of the cup shape is achieved by observing color and texture variations in the image.

Annotation procedure for RNFL in OCT imaging

Figure 23 illustrates the process of annotating the RNFL and calculating its thickness in OCT imaging: 1) OCT Image quality assessment: verify the quality of the OCT image. 2) Localization of the macula and optic nerve head: identify the macula and optic nerve head based on the OCT scanning protocol. 3) Annotation of RNFL boundaries: mark the inner and outer boundaries of the RNFL. 4) Multi-angle measurement and thickness calculation: measure and compute the RNFL thickness from multiple angles.

Annotation procedure for anterior chamber angle in AS-OCT/UBM imaging

Figure 24 outlines the annotation process for the anterior chamber angle in AS-OCT/UBM imaging: 1) Perform quality inspection on AS-OCT/UBM images. 2) Identify and mark the SS. The intersection of the boundary between scleral and ciliary body tissues and the extension of

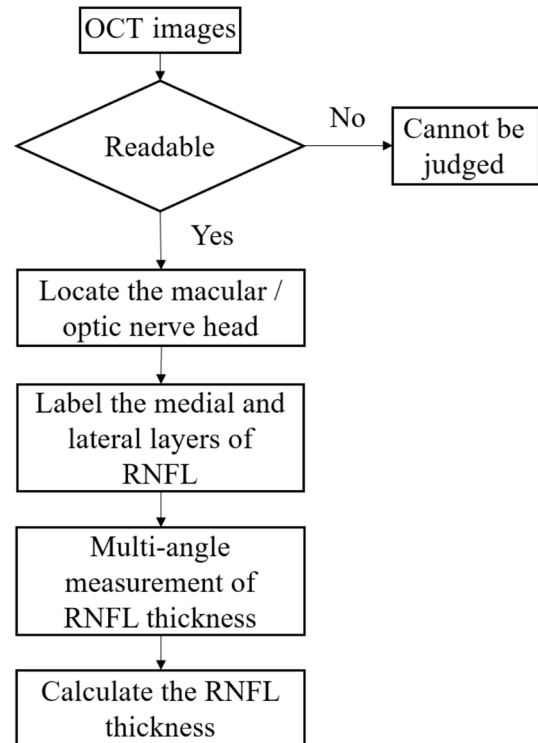


Figure 23 Annotation procedure for RNFL in OCT imaging OCT: Optical coherence tomography; RNFL: Retinal nerve fiber layer.

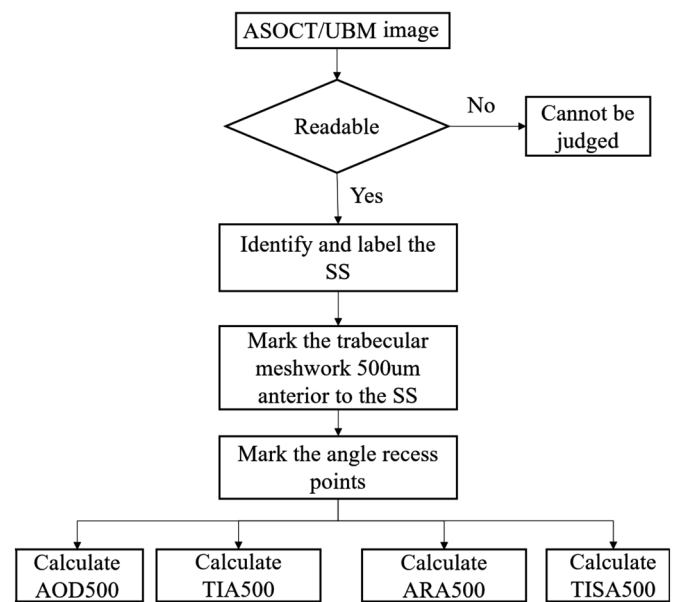


Figure 24 Annotation procedure for anterior chamber angle in ASOCT/UBM imaging ASOCT: Anterior segment optical coherence tomography; UBM: Ultrasound biomicroscopy; TIA: Trabecular iris angle; AOD: Angle opening distance; ARA: Angle recess area; TISA: Trabecular iris space area; SS: Scleral spur.

the corneal inner surface is the location of the SS^[49]. 3) Mark the trabecular meshwork point approximately 500 μm anterior to the SS on the trabecular meshwork. 4) Mark the angle recess point, which is the apex of the iris root. 5) Calculate anterior chamber angle-related parameters: AOD500, TIA500, ARA500, and TISA500.

QUALITY CONTROL REQUIREMENTS FOR GLAUCOMA IMAGING CLASSIFICATION AND ANNOTATION

Quality Control

Challenge The quality of fundus images for glaucoma varies significantly due to factors such as patient cooperation, equipment performance, and environmental conditions, which may result in blurred or unclear details.

Solutions 1) Standardize acquisition equipment and conditions: Use standardized ophthalmic imaging equipment and consistent capture conditions to minimize variability and ensure image uniformity. 2) Quality assessment tools: Develop automated or semi-automated quality assessment tools to detect issues like blurring, underexposure, and other quality defects, thereby excluding low-quality images. 3) Training for annotators: Provide professional training for annotators to accurately identify and exclude low-quality images, improving the accuracy of annotation results.

Professional Constraints

Challenge The classification of glaucoma fundus images involves multiple image types, requiring annotators to possess in-depth ophthalmological knowledge, particularly in glaucoma, to understand the complexities of various lesions in different glaucoma images.

Solutions 1) Define professional standards: Establish detailed professional standards that clearly outline the characteristics and classification criteria for lesions in various glaucoma images, providing clear guidance for annotators. 2) Annotator training: Provide annotators with necessary medical knowledge training and annotation tool training. Additionally, offer abundant real-world cases for practice, allowing annotators to develop practical skills and apply their knowledge on actual images. 3) Multi-annotator participation: Individual annotators may introduce subjective errors. To enhance annotation quality, consider using the average or integrated results from multiple annotators for the same sample to reduce individual subjectivity.

Process Supervision

Challenge Long-term annotation processes may be prone to human errors or annotation gaps, necessitating effective supervision mechanisms to improve annotation quality. Supervising the annotation process is crucial for ensuring the quality of glaucoma fundus imaging classification and annotation.

Solutions 1) Real-time feedback system: Implement a real-time feedback system to promptly identify and correct annotation errors, minimizing potential inaccuracies. 2) Regular review and training: Conduct periodic reviews of annotation and classification results to identify issues and make timely corrections. Additionally, provide regular training to

update annotators' knowledge and skills. 3) Establish an audit mechanism: Set up an independent audit mechanism where professionals review annotation and classification results to ensure accuracy and consistency.

CONCLUSION

The widespread application of AI technology in clinical practice has demonstrated remarkable potential and advantages^[50]. To enhance the diagnostic accuracy of glaucoma and facilitate the deeper integration of AI into ophthalmology, it is essential to standardize the classification, annotation methods, workflows, and quality control of glaucoma-related imaging. This guideline systematically outlines the principles and procedures for classifying and annotating multi-modal images, including CFP, OCT, AS-OCT, and UBM, providing standardized guidance for clinical and research applications. It is worth noting that some emerging imaging modalities, such as optical coherence tomography angiography (OCTA), are not included in this guideline due to their limited use and lack of consensus on classification and annotation standards in glaucoma research. Standardized classification and annotation not only enable clinicians and researchers to accurately identify and assess key pathological features related to glaucoma but also provide high-quality and structured labeled data for the training and optimization of AI models. This significantly improves the accuracy and applicability of AI in glaucoma diagnosis and promotes its clinical translation in early screening, disease monitoring, and personalized treatment. The purpose of this guideline is to unify classification and annotation protocols, standardize workflows and quality control measures, improve data consistency and comparability, and support multi-center data sharing and joint analysis. Ultimately, it aims to advance both glaucoma research and clinical practice to a higher level.

ACKNOWLEDGEMENTS

Member of the Formation Guideline Expert Group

Drafting Group Experts

| | |
|----------------|--|
| Xing-Huai Sun | Eye & ENT Hospital, Shanghai Medical College, Fudan University |
| Wei-Hua Yang | Shenzhen Eye Hospital, Shenzhen Eye Medical Center, Southern Medical University |
| Yan-Wu Xu | School of Future Technology, South China University of Technology; Pazhou Lab, Guangzhou |
| Jun-Yi Chen | Eye & ENT Hospital, Shanghai Medical College, Fudan University |
| Yuan-Bo Liang | Eye Hospital of Wenzhou Medical University |
| Jing-Min Guo | Tongji Hospital, Tongji Medical College, Huazhong University of Science and Technology |
| Gang-Wei Cheng | Peking Union Medical College Hospital |
| Yan-Long Bi | Tongji Hospital of Tongji University |
| Yu-Qing Lan | Yat-sen Memorial Hospital, Sun Yat-sen University |
| Zong-Ming Song | Henan Provincial People's Hospital, Henan Eye Hospital |

| | | | |
|---------------|---|-----------------|--|
| Jun-Ming Wang | The Second Affiliated Hospital of Guangzhou Medical University | Kai Jin | Second Affiliated Hospital, School of Medicine, Zhejiang University |
| Kai-Jun Wang | Eye Center, the 2nd Affiliated Hospital, Medical College of Zhejiang University | Gang-Jin Kang | The Affiliated Hospital of Southwest Medical University |
| Xiao-Bo Xia | Xiangya Hospital, Central South University | Li Li | Fuzhou University Affiliated Provincial Hospital |
| Hong Zhang | Eye Hospital, Harbin Medical University | Shi-Ying Li | The First Affiliated Hospital of Xiamen University, School of Medicine |
| Xuan Xiao | Renmin Hospital of Wuhan University | Xiao-Meng Li | Hong Kong University of Science and Technology |
| Li Tang | West China Hospital, Sichuan University | Xuan Liao | Affiliated Hospital, Medical School of Ophthalmology & Optometry, North Sichuan Medical College |
| Hua Zhong | The First Affiliated Hospital of Kunming Medical University | Ting Liu | Daping Hospital, Army Medical Center |
| Yang-Fan Yang | State Key Laboratory of Ophthalmology, Zhongshan Ophthalmic Center, Sun Yat-sen University | Pei-Rong Lu | The First Affiliated Hospital of Soochow University |
| Guo-Fan Cao | Eye Hospital, Nanjing Medical university | Wen-Juan Luo | Qingdao University Affiliated Hospital |
| Ying Cui | Guangdong Provincial People's Hospital (Guangdong Academy of Medical Sciences), Southern Medical University | Xiao-Fei Man | Xinhua Hospital Affiliated to Shanghai Jiao Tong University School of Medicine |
| Chao Qu | Sichuan Academy of Medical Sciences & Sichuan Provincial People's Hospital | Chu-Bin Ou | Guangdong Provincial Key Laboratory of Artificial Intelligence in Medical Image Analysis and Application |
| Min Ji | Affiliated Hospital of Nantong University | Wei-Hua Pan | Hangzhou Aier Eye Hospital |
| Li-Na Huang | Shenzhen Eye Hospital, Shenzhen Eye Medical Center, Southern Medical University | Li Sun | Affiliated Hospital of Integrated Traditional Chinese and Western Medicine, Nanjing University of Chinese Medicine |
| Jian-Tao Wang | Shenzhen Eye Hospital, Shenzhen Eye Medical Center, Southern Medical University | Wen Sun | Children's Hospital, Zhejiang University School of Medicine |
| Yi Shao | Shanghai General Hospital, Shanghai Jiao Tong University School of Medicine | Guang-Xian Tang | Shijiazhuang People's Hospital |
| Hui-Hui Fang | Pazhou Lab, Guangzhou | Li-Ming Tao | The Second Affiliated Hospital of Anhui Medical University |
| Qiu-Shi Ren | Department of Biomedical Engineering, Peking University | Yu-Hua Tong | The Quzhou Affiliated Hospital of Wenzhou Medical University, Quzhou People's Hospital |

Participating Expert Reviewers (Listed in Alphabetical Order by Surname)

| | | | |
|---------------|--|-----------------|---|
| Xin-Jian Chen | Soochow University | Cheng Wan | Nanjing University of Aeronautics and Astronautics |
| Qin Chen | The First Affiliated Hospital with Nanjing Medical University | Hai-Yan Wang | Shanghai General Hospital, Shanghai Jiao Tong University School of Medicine |
| Wei-Wei Dai | Aier Institute of Digital Ophthalmology & Visual Science | Meng Wang | National University of Singapore |
| Da-Yong Ding | Visionary Intelligence Ltd. | Shu-Jun Wang | The Hong Kong Polytechnic University |
| Lin Ding | People's Hospital of Xinjiang Uygur Autonomous Region | Xian Wang | The Affiliated Hospital of Guizhou Medical University |
| Xi-Yan Ding | Eye Hospital, Nanjing Medical University | Xiao-Yu Wang | The First Affiliated Hospital, Zhejiang University School of Medicine |
| Shao-Lin Du | Dongguan Tungwah Hospital | Rui-Li Wei | Shanghai Changzheng Hospital |
| Li-Xin Duan | Shenzhen Institute for Advanced Study, University of Electronic Science and Technology of China | Yu-Bo Wei | Beijing Airdoc Technology Co., Ltd. |
| Hua-Zhu Fu | Institute of High Performance Computing, Agency for Science, Technology and Research (A*STAR), Singapore | Zheng-Gao Xie | Nanjing Drum Tower Hospital, the Affiliated Hospital of Medical School, Nanjing University |
| Peng Gao | Shanghai Tenth People's Hospital of Tongji University | Fan Xu | The People's Hospital of Guangxi Zhuang Autonomous Region & Guangxi Academy of Medical Sciences |
| Wei Han | Second Affiliated Hospital, School of Medicine, Zhejiang University | Xiao-Ping Xu | Ningbo Eye Hospital |
| Jian-Zhang Hu | Fujian Medical University Union Hospital | Qi-Bin Xu | Zhejiang Hospital of Integrated Traditional Chinese and Western Medicine |
| Ke Hu | The First Affiliated Hospital of Chongqing Medical University | Yong-Sheng Yang | Eye Hospital, China Academy of Chinese Medical Sciences |
| Man Hu | Beijing Children's Hospital, Capital Medical University | Xue Yao | Shenzhen Eye Hospital, Shenzhen Eye Medical Center, Southern Medical University |
| Yong-Ping Hu | Affiliated Hangzhou First Peoples Hospital, School of Medicine, Westlake University | Zhen-Yu Yao | Affiliated Hospital of Inner Mongolia University for the Nationalities |
| Chu-Kai Huang | Joint Shantou International Eye Center of Shantou University & the Chinese University of HongKong | Li-Jing Yue | Guangdong Second Traditional Chinese Medicine Hospital |
| Hou-Bin Huang | Senior Department of Ophthalmology, PLA General Hospital | Dong-Dong Zhang | Beijing Zhenhealth Technology Co., Ltd. |
| Yi-Ping Jiang | The First Affiliated Hospital of Gannan Medical University | Guang-Hua Zhang | Taiyuan University |
| | | Hong-Yang Zhang | Nanfeng Hospital, Southern Medical University |
| | | Jiong Zhang | Ningbo Institute of Materials Technology and Engineering, Chinese Academy of Sciences (CAS) |

| | |
|----------------------|--|
| Wen-Song Zhang | The Second Hospital of Jilin University |
| Jun Zhao | Shenzhen People's Hospital |
| Yi-Tian Zhao | Ningbo Institute of Materials Technology and Engineering, Chinese Academy of Sciences (CAS) |
| Bo Zheng | Huzhou University |
| Guo-Hong Zhou | Shanxi Eye hospital |
| Sheng Zhou | Institute of Biomedical Engineering, Chinese Academy of Medical Science and Peking Union Medical College |
| Yong-Jin Zhou | Shenzhen University |
| Ya-Lin Zheng | University of Liverpool, St Paul's Eye Unit, Royal Liverpool University Hospital (UK) |
| Neeru Amrita Vallabh | University of Liverpool, St Paul's Eye Unit, Royal Liverpool University Hospital (UK) |
| Stephen Kaye | St Paul's Eye Unit, Royal Liverpool University Hospital, University of Liverpool (UK) |
| Vito Romano | University of Brescia (Italy) |
| Colin Willoughby | Ulster University (UK) |

Secretaries of the Expert Group

| | |
|----------------|--|
| Wei Lu | Eye & ENT Hospital, Shanghai Medical College, Fudan University |
| Yue Wu | Shanghai Ninth People's Hospital, Shanghai Jiao Tong University School of Medicine |
| Jing-Yuan Yang | Peking Union Medical College Hospital |
| Di Gong | Shenzhen Eye Hospital, Shenzhen Eye Medical Center, Southern Medical University |

Guideline Statement This guideline was drafted by experts in the field of glaucoma imaging classification, annotation methods, workflows, and quality control. All participating experts have maintained an objective and impartial stance, formulating the guideline based on existing scientific research evidence, professional knowledge, and clinical experience after thorough discussion. The development process adhered to the principles of scientific rigor, practicality, and consistency, aiming to provide standardized guidance for glaucoma imaging classification, annotation methods, workflows, and quality control, while promoting the application and advancement of AI technology in ophthalmology.

Disclaimer The content of this guideline represents the professional recommendations of the expert group on glaucoma imaging classification and annotation, serving as a reference for clinicians and researchers. While extensive discussions and consultations were conducted during the development process, certain aspects may still require further refinement. The recommendations in this guideline are non-mandatory, and deviations from them should not necessarily be considered erroneous or inappropriate. In intelligent ophthalmic clinical practice, many aspects of glaucoma imaging classification, annotation methods, workflows, and quality control still require further exploration. As clinical experience accumulates and related technologies advance, periodic updates and revisions will be necessary to ensure the

guideline remains current and continues to provide greater clinical benefits for patients.

Foundations: Supported by Guangdong Basic and Applied Basic Research Foundation (No.2025A1515011627); San Ming Project of Medicine in Shenzhen (No.SZSM202311012).
Conflicts of Interest: Yang WH, None; Xu YW, None; Sun XH, None; **Expert Workgroup of Guidelines for Glaucoma Imaging Classification, Annotation, and Quality Control for Artificial Intelligence Applications**, None.

REFERENCES

- 1 Wang X, Chao QU. Recent advances in pathogenesis and treatment of optic nerve injury in glaucoma. *Recent Advances in Ophthalmology* 2024;44(7):572-577.
- 2 Zhang LY, Tang L, Xia M, *et al.* The application of artificial intelligence in glaucoma diagnosis and prediction. *Front Cell Dev Biol* 2023;11:1173094.
- 3 Jia QF, Wang XF, Li XW, *et al.* Analysis of research hotspots and trends in pediatric ophthalmopathy based on 10 years of WoSCC literature. *Front Pediatr* 2024;12:1405110.
- 4 Yang WH, Shao Y, Xu YW, *et al.* Guidelines on clinical research evaluation of artificial intelligence in ophthalmology (2023). *Int J Ophthalmol* 2023;16(9):1361-1372.
- 5 Wu JD, Fang HH, Zhu JY, *et al.* Multi-rater prism: learning self-calibrated medical image segmentation from multiple raters. *Sci Bull (Beijing)* 2024;69(18):2906-2919.
- 6 Li HS, Lyu X, Zhang J, *et al.* Opportunities and challenges in the establishment of the digital ophthalmological care model. *Digital Medicine and Health* 2024;2(4):213-218.
- 7 Chen JS, Lin WC, Yang S, *et al.* Development of an open-source annotated glaucoma medication dataset from clinical notes in the electronic health record. *Transl Vis Sci Technol* 2022;11(11):20.
- 8 Cui N, Jia J, He Y. Glaucomatous retinal ganglion cells: death and protection. *Int J Ophthalmol* 2025;18(1):160-167.
- 9 Qian CX. Research progress of artificial intelligence in glaucoma. *Guoji Yanke Zazhi (Int Eye Sci)* 2021;21(12):2081-2085.
- 10 Chen JY, Sun XH. Highlights of terminology and guidelines for glaucoma (5th edition): an interpretation. *Chin J Exp Ophthalmol* 2021;39(10):906-909.
- 11 Kim J, Tran L, Peto T, *et al.* Identifying those at risk of glaucoma: a deep learning approach for optic disc and cup segmentation and their boundary analysis. *Diagnostics (Basel)* 2022;12(5):1063.
- 12 Alawad M, Aljouie A, Alamri S, *et al.* Machine learning and deep learning techniques for optic disc and cup segmentation - a review. *Clin Ophthalmol* 2022;16:747-764.
- 13 China Association for Quality Inspection. Annotation and quality control specifications for fundus color photograph. *Intell Med* 2021;1(2):80-87.
- 14 Tan O, Liu L, You QS, *et al.* Focal loss analysis of nerve fiber layer reflectance for glaucoma diagnosis. *Transl Vis Sci Technol* 2021;10(6):9.

- 15 Jin SW, Bouris E, Morales E, *et al.* Long-term rate of optic disc rim loss in glaucoma patients measured from optic disc photographs with a deep neural network. *Transl Vis Sci Technol* 2024;13(9):9.
- 16 Maupin E, Baudin F, Arnould L, *et al.* Accuracy of the ISNT rule and its variants for differentiating glaucomatous from normal eyes in a population-based study. *Br J Ophthalmol* 2020;104(10):1412-1417.
- 17 Harwerth RS, Quigley HA. Visual field defects and retinal ganglion cell losses in patients with glaucoma. *Arch Ophthalmol* 2006;124(6):853-859.
- 18 Hood DC, Bruna SL, Tsamis E, *et al.* Detecting glaucoma with only OCT: implications for the clinic, research, screening, and AI development. *Prog Retin Eye Res* 2022;90:101052.
- 19 Nishida T, Moghimi S, Chang AC, *et al.* Association of intraocular pressure with retinal nerve fiber layer thinning in patients with glaucoma. *JAMA Ophthalmol* 2022;140(12):1209-1216.
- 20 Lingham G, Lee SS, Charn J, *et al.* Distribution and classification of peripapillary retinal nerve fiber layer thickness in healthy young adults. *Transl Vis Sci Technol* 2021;10(9):3.
- 21 Alasil T, Wang KD, Yu F, *et al.* Correlation of retinal nerve fiber layer thickness and visual fields in glaucoma: a broken stick model. *Am J Ophthalmol* 2014;157(5):953-959.
- 22 Christopher M, Bowd C, Proudfoot JA, *et al.* Performance of deep learning models to detect glaucoma using unsegmented radial and circle OCT scans of the optic nerve head. *Investigative Ophthalmology & Visual Science* 2021;62(8):1014.
- 23 Gupta A, Bansal R, Sharma A, *et al.* Optic disc signs—cupping, swelling, inflammation, and pallor. *Ophthalmic Signs in Practice of Medicine*. Singapore: Springer Nature Singapore, 2023:423-472.
- 24 Kan JT, Betzler BK, Lim SY, *et al.* Anterior segment imaging in minimally invasive glaucoma surgery—a systematic review. *Acta Ophthalmol* 2022;100(3):e617-e634.
- 25 Lippera M, Nicolosi C, Vannozzi L, *et al.* The role of anterior segment optical coherence tomography in uveitis-glaucoma-hyphema syndrome. *Eur J Ophthalmol* 2022;32(4):2211-2218.
- 26 Sihota R, Shakrawal J, Sidhu T, *et al.* Does trabeculectomy meet the 10-10-10 challenge in PACG, POAG, JOAG and secondary glaucomas? *Int Ophthalmol* 2020;40(5):1233-1243.
- 27 Cheung CY, Li SL, Chan PP, *et al.* Intraocular pressure control and visual field changes in primary angle closure disease: the CUHK PACG Longitudinal (CUPAL) study. *Br J Ophthalmol* 2020;104(5):629-635.
- 28 Foster PJ, Johnson GJ. Glaucoma in China: how big is the problem? *Br J Ophthalmol* 2001;85(11):1277-1282.
- 29 Zhang N, Wang JX, Li Y, *et al.* Prevalence of primary open angle glaucoma in the last 20 years: a meta-analysis and systematic review. *Sci Rep* 2021;11(1):13762.
- 30 Zhang N, Wang JX, Chen BY, *et al.* Prevalence of primary angle closure glaucoma in the last 20 years: a meta-analysis and systematic review. *Front Med (Lausanne)* 2020;7:624179.
- 31 Scheie HG. Width and pigmentation of the angle of the anterior chamber; a system of grading by gonioscopy. *AMA Arch Ophthalmol* 1957;58(4):510-512.
- 32 Samaha D, Gagné S, Corbeil ME, *et al.* Predicting the risk for angle closure as defined by the Shaffer system using anterior segment optical coherence tomography: a simple approach. *Can J Optom* 2020;82(1):100-105.
- 33 van Herick W, Shaffer RN, Schwartz A. Estimation of width of angle of anterior chamber. Incidence and significance of the narrow angle. *Am J Ophthalmol* 1969;68(4):626-629.
- 34 Riva I, Micheletti E, Oddone F, *et al.* Anterior chamber angle assessment techniques: a review. *J Clin Med* 2020;9(12):3814.
- 35 Ong AY, Ng SM, Vedula SS, *et al.* Lens extraction for chronic angle-closure glaucoma. *Cochrane Database Syst Rev* 2021;3:CD005555.
- 36 Janssens R, van Rijn LJ, Eggink CA, *et al.* Ultrasound biomicroscopy of the anterior segment in patients with primary congenital glaucoma: a review of the literature. *Acta Ophthalmol* 2022;100(6):605-613.
- 37 Ishikawa H, Esaki K, Liebmann JM, *et al.* Ultrasound biomicroscopy dark room provocative testing: a quantitative method for estimating anterior chamber angle width. *Jpn J Ophthalmol* 1999;43(6):526-534.
- 38 Esaki K, Ishikawa H, Liebmann JM, *et al.* Angle recess area decreases with age in normal Japanese. *Jpn J Ophthalmol* 2000;44(1):46-51.
- 39 Wang XW, Wang Y, Wang CJ, *et al.* Glaucoma diagnosis and prediction based on multi-scale feature coding. *2023 IEEE International Conference on Image Processing and Computer Applications (ICIPCA)*. August 11-13, 2023, Changchun, China. IEEE, 2023:822-831.
- 40 Wu JD, Fang HH, Wang ZW, *et al.* Learning self-calibrated optic disc and cup segmentation from multi-rater annotations. *Medical Image Computing and Computer Assisted Intervention—MICCAI 2022*. Cham: Springer Nature Switzerland, 2022:614-624.
- 41 Ocular Fundus Diseases Group of Chinese Ophthalmological Society; Expert Group for Artificial Intelligence Research, Development, and Application. The standardized design and application guidelines: a primary-oriented artificial intelligence screening system of the lesion sign in the macular region based on fundus color photography. *Intell Med* 2023;3(3):213-227.
- 42 Bowd C, Weinreb RN, Williams JM, *et al.* The retinal nerve fiber layer thickness in ocular hypertensive, normal, and glaucomatous eyes with optical coherence tomography. *Arch Ophthalmol* 2000;118(1):22-26.
- 43 Bai JH, Wan ZQ, Li P, *et al.* Accuracy and feasibility with AI-assisted OCT in retinal disorder community screening. *Front Cell Dev Biol* 2022;10:1053483.
- 44 Wu JH, Moghimi S, Nishida T, *et al.* Association of macular OCT and OCTA parameters with visual acuity in glaucoma. *Br J Ophthalmol* 2023;107(11):1652-1657.
- 45 Ghadamzadeh M, Karimi F, Ghasemi Moghaddam S, *et al.* Anterior chamber angle changes in primary angle-closure glaucoma following

- phacoemulsification versus phacotrabeculectomy: a prospective randomized clinical trial. *J Glaucoma* 2022;31(3):147-155.
- 46 Sosnowik S, Swain DL, Liu N, *et al.* Endothelial glycocalyx morphology in different flow regions of the aqueous outflow pathway of normal and laser-induced glaucoma monkey eyes. *Cells* 2022;11(15):2452.
- 47 Zhang M, An GQ, Liu P, *et al.* Correlation between axial lengths and anterior segment parameters evaluated by swept-source optical coherence tomography. *Guoji Yanke Zazhi (Int Eye Sci)* 2023;23(8):1338-1342.
- 48 Lei CY, Wang H, Zhao C, *et al.* Standards in the collection of facial images for the diagnosis and assessment of ocular diseases. *Digital Medicine and Health* 2024;2(4):219-223.
- 49 Fu Y, Jiang B, Liu Y, *et al.* Anterior segment anatomic parameters based on the scleral spur and cornea for risk profiling of primary angle closure glaucoma. *Ophthalmic Res* 2025;68(1):228-236.
- 50 Yang WH, Fang HH, Wang SJ, *et al.* Artificial intelligence empowers ophthalmology clinic: transforming algorithms into medical assistants. *Digital Medicine and Health* 2024;2(4):209-212.